Diagn Interv Radiol 2009; 15:172–175
© Turkish Society of Radiology 2009

18F-FDG PET-CT features of primary primitive neuroectodermal tumor of the chest wall

Mustafa Kemal Demir, Filiz Koşar, Yasemin Sanlı, Safa Esmaeilzadeh, Halide Nur Ürer

ABSTRACT
A case of primary primitive neuroectodermal tumor (PNET) of the chest wall in an adolescent is presented with imaging findings including 18F-fluorodeoxyglucose (18F-FDG) positron-emission computed tomography (PET-CT). To date, radiological description of the PNET of the chest wall has mainly been carried out by radiographic analysis, computed tomography (CT), and magnetic resonance imaging (MRI). We demonstrated that 18F-FDG PET-CT visualizes the active focus of glucose metabolism of PNET of the chest wall and is effective for the preoperative evaluation of patients with this tumor.

Key words: • *fluorodeoxyglucose F18* • *positron-emission tomography* • *neuroectodermal tumors, primitive*

A primitive neuroectodermal tumor (PNET) of thoracoabdominal region is one of a group of small round cell tumors usually found in children and young adults. It was originally described by Askin et al. (1), and it is associated with a chromosome 22 translocation. Most cases arise in the soft tissues of the thorax; they may rarely occur within the lung (2). The most common presenting symptom is chest wall pain, which can be accompanied by a pleural effusion and dyspnea. We report the imaging features, including 18F-fluorodeoxyglucose (18F-FDG) positron-emission computed tomography (PET-CT), of a PNET of the chest wall in a 17-year-old male and discuss the differential diagnosis.

Case report

A 17-year-old male was admitted to the hospital with recent onset of continuous, worsening pain in the upper part of his right chest. He was afebrile. Physical examination revealed tenderness to palpation of the posterior part of upper right hemithorax. Findings of laboratory tests were unremarkable. Digital scout chest radiography (Fig. 1) revealed a well-defined, round, homogeneous opacity projecting over the right lung apex, with deviation of the trachea and mediastinum to the left. Computed tomography (CT) of the chest (Fig. 2) showed a 10 × 10 × 8 cm circumscribed soft tissue mass within the right upper hemithorax, arising from the chest wall. The adjacent posterior rib was directly affected by the lesion. The lung areas were clear. The mass was heterogeneously hyperintense to the skeletal muscle on T2-weighted magnetic resonance (MR) image (Fig. 3a), and hypointense on T1-weighted MR image (Fig. 3b). Magnetic resonance imaging (MRI) performed after intravenous administration of gadolinium contrast material showed heterogeneous enhancement of the mass (Fig. 3c). There was extension of the tumor to the ribs and chest wall soft tissues. No lymphadenopathy was identified. Fine-needle aspiration biopsy was done to provide a histopathological diagnosis. Cytological examination of the biopsy specimen revealed a malignant small round cell tumor (Fig. 4a). On immunocytochemical staining, tumor cells were stained positively only for synaptophysin (Fig. 4b) and were negative for leukocyte common antigen (CD45), CD56, CD99, vimentin, pancytokeratin, epithelial membrane antigen (EMA), chromogranin A, and thyroid transcription factor-1. Although the tumor in this case was negative for CD99, CD56, and chromogranin A, the histopathological results combined with the imaging findings and patient's age led to a diagnosis of PNET of the chest wall. Whole-body integrated PET-CT for tumor staging demonstrated intense and homogeneous 18F-FDG uptake in the right hemithoracic mass (Fig. 5). Standardized uptake value (SUV) was 8.3. There were no abnormal hypermetabolic foci elsewhere in the body.

From the Department of Radiology (M.K.D. ✉ *demirkemal@superonline.com*), Trakya University School of Medicine, Edirne, Turkey; the Department of Chest Diseases (F.K.), and Pathology (H.N.Ü.), Yedikule Teaching Hospital for Chest Diseases and Thoracic Surgery, İstanbul, Turkey; and the Divisions of Nuclear Medicine (Y.S.), and Radiology (S.E.), Starmar Imaging Center, İstanbul, Turkey.

Received 5 April 2007; revision requested 4 December 2007; revision received 5 December 2007; accepted 30 December 2007.

Figure 1. Digital scout chest radiography reveals a large well-circumscribed homogeneous opacity in the right upper zone and leftward deviation of the trachea.

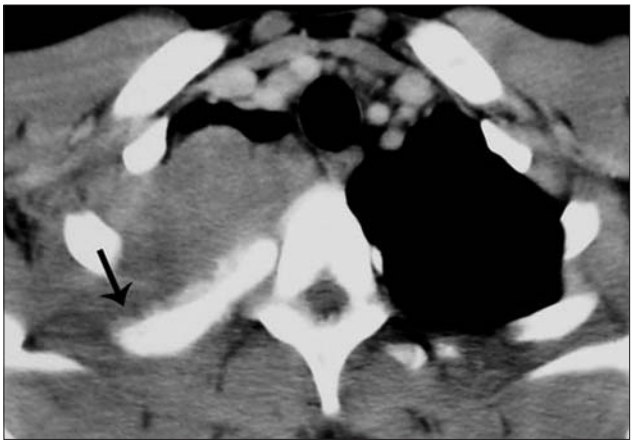

Figure 2. Axial contrast-enhanced CT section of the chest shows a large solid mass in the upper right hemithorax. Note the hyperostosis and backward displacement of the third rib *(arrow)*.

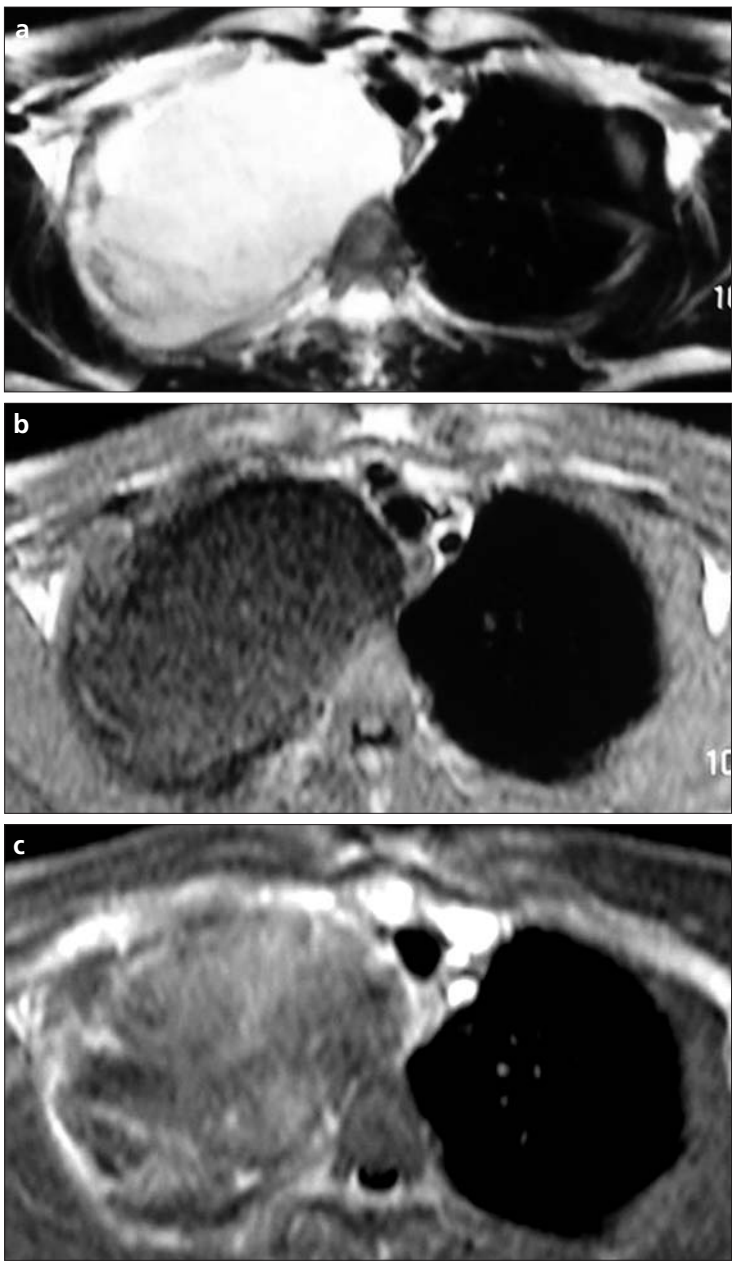

Figure 3. a–c. Transverse T2-weighted **(a)**, T1-weighted **(b)**, and contrast-enhanced fat-suppressed T1-weighted **(c)** MR images. T2-weighted MR image **(a)** shows a large mass of heterogeneous high signal intensity in the right hemithorax. The mass is hypointense on transverse T1-weighted image **(b)**, and shows moderate enhancement on contrast-enhanced fat-suppressed T1-weighted image **(c)**.

Discussion

PNET of the chest wall, or Askin tumor, is a malignant tumor of the Ewing family of tumors comprising small, undifferentiated neuroectodermal cells. The Ewing family of tumors also include Ewing sarcoma of bone, extraosseous Ewing sarcoma, and peripheral neuroepithelioma. These rare tumors are considered to arise from a common origin, neuroectoderm, in which malignant cells are found in bone and soft tissues; they most frequently occur in teenagers.

The imaging evaluation of a PNET of the chest wall requires a multimodality approach. Chest radiography is the first study that would be performed in a patient with symptoms referable to the thorax. It usually demonstrates an intrathoracic extraparenchymal mass, with extrathoracic extension and rib involvement. CT examination of the chest is useful for the diagnosis of rib involvement, lung infiltration, and lung metastasis in these patients. MRI is the preferred modality in the presence of a large chest wall mass. It provides superior soft tissue contrast and allows multiplanar image acquisition, resulting in a clear assessment of chest wall soft tissue involvement. Pleural invasion and effusion can also be clearly evaluated by MRI (3). How-

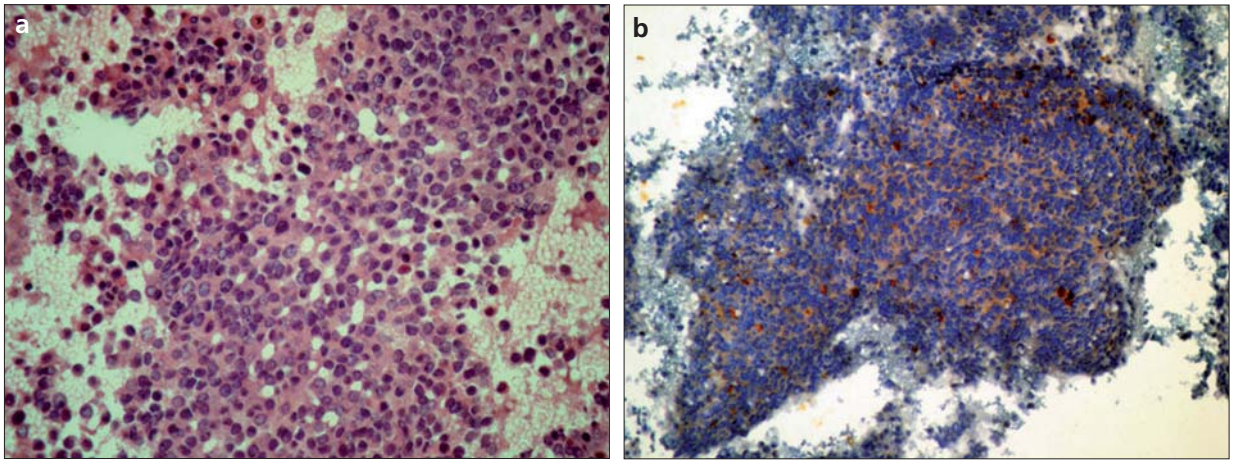

Figure 4. a, b. Digital photomicrographs of the tumor **(a, b)**. Proliferation of small round cells with very scant cytoplasm and fine chromatin pattern is seen **(a)** (original magnification, x400; hematoxylene-eosin stain). Tumor cells showed strong immunoreactivity **(b)** (original magnification, x200; synaptophysin stain).

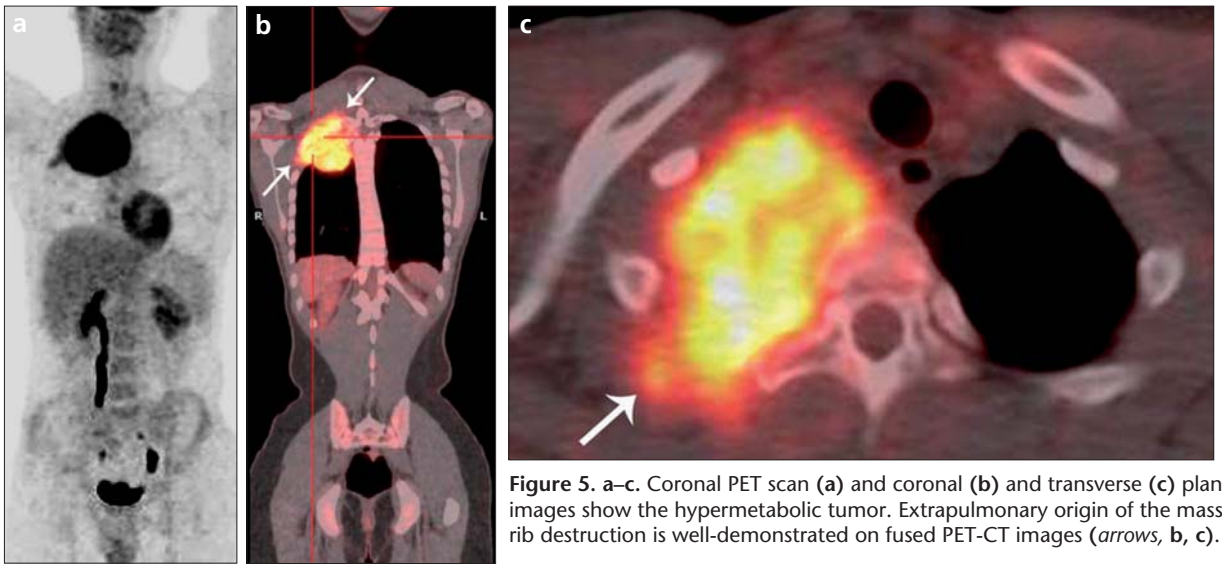

Figure 5. a–c. Coronal PET scan **(a)** and coronal **(b)** and transverse **(c)** plane fused PET-CT images show the hypermetabolic tumor. Extrapulmonary origin of the mass with posterior rib destruction is well-demonstrated on fused PET-CT images **(***arrows,* **b, c)**.

ever, it should be emphasized that CT and MRI cannot always reliably distinguish between benign and malignant chest wall soft tissue masses.

FDG is a metabolic tracer avidly accumulated in cancer cells. FDG PET has been suggested as a complement to CT and MRI in the staging of sarcomas (4, 5). It has the potential to discriminate between sarcomas and benign tumors, as well as between low- and high-grade sarcomas. However, the role of PET-CT using FDG in the diagnostic work-up of PNET of the chest wall has not yet been clearly established. There are several reports describing the FDG uptake of PNET in the literature, but none of the patients had PNET of the chest wall. Unfortunately, these reports contain contradictory imaging findings. Although there was increased FDG uptake demonstrating intense hypermetabolism of the tumor (5–7), a case of PNET of the right upper extremity did not show FDG uptake despite its large size and aggressive nature (8). This contradiction may be attributed to the differences in biological behaviour and metabolic profiles of PNET in different sites. It is suggested that the reason for absence of FDG uptake by a variety of malignant tumors is the underexpression of Glut-1 transporter and/or hexokinase II enzymes, which phosphorylate glucose to glucose-6-phosphate (8).

When an increased FDG uptake exists, fused PET-CT shows direct tumor invasion into chest wall structures better than other imaging modalities, as in our case. The ability to provide imaging in all three planes also helps demonstrate the extent of disease and determine resectability.

SUV is defined as the ratio of activity of tissue per milliliter to the activity in the injected dose, corrected for decay and patient's body weight, lean body mass, or body surface area. Although it has been suggested that SUV measurements can help successfully discriminate between benign and malignant tumors, it is not uncommon to see overlap in the values. Malignant soft tissue sarcomas sometimes show low FDG uptake and benign lesions high uptake (9). Practically, all intermediate/high-grade soft tissue sarcomas have SUV ≥2.0, which correlates

well with the SUV value of the current case.

The differential diagnosis of PNET of the chest wall may include Ewing sarcoma, chondrosarcoma, malignant fibrous histiocytoma, osteosarcoma, and fibrosarcoma (10). Differences in clinical presentation, location of the tumor, rib involvement, presence of calcification or ossification, and imaging characteristics, including FDG PET-CT findings, can provide the correct diagnosis in most cases.

In conclusion, we presented a case of PNET of the chest wall with imaging findings, including FDG PET-CT, which have not been previously reported. This case demonstrates that 18F-FDG PET-CT visualizes the active focus of glucose metabolism of PNET of the chest wall and is effective for the preoperative evaluation of a patient with this tumor. The image demonstrating preoperative intense FDG uptake of the mass is also useful as a baseline imaging study for monitoring these patients.

References

1. Askin FB, Rosai J, Sibley RK, Dehner LP, McAlister WH. Malignant small cell tumor of the thoracopulmonary region in childhood: a distinctive clinicopathologic entity of uncertain histogenesis. Cancer 1979; 43:2438–2451.
2. Paik SH, Park JS, Koh ES, et al. Primary pulmonary primitive neuroectodermal tumor: CT and skeletal scintigraphic image features with pathologic correlation (2006: 6b). Eur Radiol 2006; 16:2128–2131.
3. Sallustio G, Pirronti T, Lasorella A, Natale L, Bray A, Marano P. Diagnostic imaging of primitive neuroectodermal tumour of the chest wall (Askin tumour). Pediatr Radiol 1998; 28:697–702.
4. Lucas JD, O'Doherty MJ, Wong JC, et al. Evaluation of FDG PET in the management of soft tissue sarcomas. J Bone Joint Surg 1998; 80:441–447.
5. Gyorke T, Zajic T, Lange A, Schafer O, Moser E, Mako E, Brink I. Impact of FDG PET for staging of Ewing sarcomas and primitive neuroectodermal tumours. Nucl Med Commun 2006; 27:17–24.
6. Meltzer CC, Townsend DW, Kottapally S, Jadali F. FDG imaging of spinal cord primitive neuroectodermal tumor. J Nucl Med 1998; 39:1207–1209.
7. Watanabe N, Kawano M, Takada M, et al. F-18 FDG PET imaging in a primitive neuroectodermal tumor. Clin Nucl Med 2006; 31:484–485.
8. Musana KA, Raja S, Cangelosi CJ, Lin YG. FDG PET scan in a primitive neuroectodermal tumor. Ann Nucl Med 2006; 20:221–225.
9. Ioannidis JP, Lau J. 18F-FDG PET for the diagnosis and grading of soft-tissue sarcoma: a meta-analysis. J Nucl Med 2003; 44:717–724.
10. Gladish GW, Sabloff BM, Munden RF, Truong MT, Erasmus JJ, Chasen MH. Primary thoracic sarcomas. Radiographics 2002; 22:621–637.